Tropospheric Oxidation of Ethyne and But-2-yne. 1. Theoretical Mechanistic Study

Andrea Maranzana,[†,‡] Giovanni Ghigo,[†] Glauco Tonachini,*[,†] and John R. Barker[‡]

Dipartimento di Chimica Generale e Chimica Organica, Università di Torino, Corso Massimo D'Azeglio 48, I-10125 Torino, Italy, and Department of Atmospheric, Oceanic, and Space Sciences, 1520 Space Research Building, 2455 Hayward Street, University of Michigan, Ann Arbor, Michigan 48109-2143

Received: September 6, 2007; In Final Form: January 25, 2008

This paper (part 1) and the following one (part 2) aim to assess the viability of some tropospheric oxidation channels for two symmetrical alkynes, ethyne (acetylene) and but-2-yne. Paper 1 defines the features of the DFT(B3LYP)/6-311G(3df,2p) energy hypersurface and qualitatively considers the practicability of different pathways through the estimate of free energy barriers. Paper 2 will assess this in more detail by way of master equation simulations. Oxidized in the presence of HO and O_2 (with the possible intervention of NO), ethyne and but-2-yne are known to produce mainly glyoxal or dimethylglyoxal and, to a lesser extent, formic or acetic acid. The initial attack by HO gives an adduct, from which several pathways (**1a**−**c**, **2a**−**e**) originate. Pathway **1a** passes through the 2-oxoethyl (vinoxyl) radical, or the analogous dimethyl-substituted intermediate, which could in principle undergo O_2 addition (and subsequently, but through a demanding step, give the dialdehydes). However, in paper 2 it is assessed that the vinoxyl, as a nonthermalized intermediate, will preferentially follow unimolecular pathways to ketene or acetyl. Pathway **2a** is the most important pathway: a very steep free energy cascade, started by O_2 addition to the initial HO adduct with a concerted barrierless 1,5 H shift, gives a hydroperoxyalkenyloxyl radical intermediate. Peroxy bond cleavage finally produces the dialdehydes and regenerates HO. Pathways **2b** and **2c** originate from O_2 addition to the initial HO adduct and produce, via different ring closures, either dioxetanyl or alkyl dioxiranyl radicals, respectively. Two subsequent fragmentations occur in both cases and give the carboxylic acids and a carbonyl radical, which can indirectly generate hydroxyl. Two further pathways (**1c** and **2e**) see NO intervention onto the peroxyl radicals formed along pathways **1** and **2**. Both could enhance dialdehyde production, while simultaneously depressing the carboxylic acid yield.

Introduction

The simplest alkynes are present in trace amounts in gasoline and their presence in the atmosphere has been observed even in remote regions.[1] Like other volatile unsaturated organic compounds of biogenic or anthropogenic nature, they usually undergo a variety of oxidative transformations in the troposphere. Their degradation pathways can be characterized by unimolecular steps and bimolecular reactions involving small free radicals like HO, NO, or O_2, in bimolecular steps. These small radicals exhibit variable and dissimilar concentrations, and different reactivities.[2,3] Thus, the environmental conditions, namely temperature and concentration variations, can in principle modulate the relative importance of possibly competing alkyne oxidation pathways.

Alkyne oxidation has been the subject of a number of experimental studies, most of them focused on ethyne (acetylene). The main loss of alkynes is due to reaction with hydroxyl.[3] Both the pressure dependence of the rate constants and their values indicate that the first step involves the formation of an addition intermediate product **I**.[4−6] As the main products are dicarbonyls **II** (see for instance Table 2 in ref 7), the reaction in Scheme 1 was postulated.[3,5,6] Carboxylic acids **III** are also detected, namely formic acid for ethyne (30−50% yield) and propyne (10−14% yield), and acetic acid for but-2-yne (11−13% yield).[6]

SCHEME 1

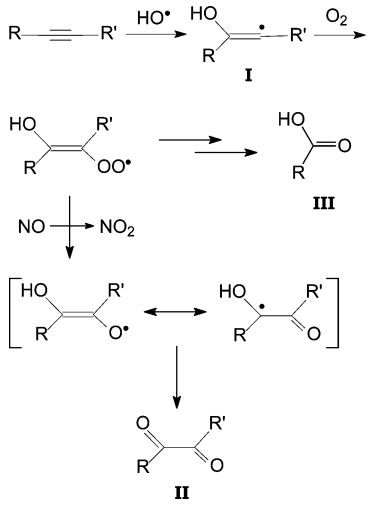

A biexponential HO decay was observed by Becker and co-workers,[5] and was attributed to fast secondary reactions. More precisely, OD formation in the reaction HO + C_2D_2 was observed and attributed to a fast reaction of the primary adduct with dioxygen.[5] Zetzsch and co-workers also observed a biexponential decay, and proposed that the initial hydroxyl

* Corresponding author. E-mail: glauco.tonachini@unito.it. Fax: ++39−011−236.7648.
† Università di Torino.
‡ University of Michigan.

10.1021/jp077174o CCC: $40.75
Published on Web 03/18/2008

adduct **I**, when reacting with dioxygen, reacts via two pathways, one of which generates the dicarbonyl product **II** and hydroxyl over again.[7]

Schmidt et al.,[5] having observed by a laser induced fluorescence (LIF) technique the vinoxyl radical [O═CH−CH_2• ↔ •O−CH═CH_2] for ethyne, suggested that the initial adduct **I** can isomerize through a hydrogen shift from the hydroxyl oxygen to the distal carbon. Its fast reaction with dioxygen, which ultimately leads to formation of glyoxal, delayed with respect to the disappearance of the vinoxyl radical itself, suggested in turn to Zhu and Johnston that the further evolution of the peroxyl radical CHO−CH_2−OO• could explain these results.[8] However, the dicarbonyl yield in the reaction of the vinoxyl radical (generated by photolysis of methyl vinyl ether) was found to be only 10−20% by Gutman and Nelson.[9] This result contrasts with the 40−100% yield observed by Hatakeyama et al. in the reaction of ethyne,[6] suggesting that more than one channel contributes to the formation of glyoxal from ethyne.[9] More recently, Delbos et al.[10] have generated the vinoxyl radical and studied the kinetics of its evolution in the presence of oxygen, both experimentally, over an extended pressure and temperature range, and theoretically, by quantum chemical calculations and master equation simulations. Also Kuwata et al.[11] have recently investigated the oxidation of vinoxyl radicals by quantum chemical methods followed by master equation simulations.

An experimental kinetic study, accompanied by MG2MS and DFT(B3LYP) computations (B3LYP for short in the following), was carried out recently by Yeung, Pennino, Miller, and Elrod (YPME)[12] on ethyne, but-2-yne, and propyne. Two other theoretical kinetic studies[13,14] on the reaction of HO with ethyne have been recently carried out by different quantum mechanical methods, with subsequent use of a Master Equation method to assess the kinetic behavior. The quantum mechanical methods used by Senosiain, Klippenstein, and Miller (SKM)[13] range from B3LYP, used to determine stable and transition structures, to restricted Quadratic CI, used to reassess the energies. Similarly, Pilling and co-workers[14] used B3LYP to define the geometries of the species involved, then recalculated the energies by the composite CBS-QCI/APNO method.

In the present paper (paper 1), we have undertaken the study of several tropospheric oxidation pathways for the simplest symmetrical alkynes: ethyne and but-2-yne. Work is in progress for the less symmetric homologues propyne and but-1-yne which present a larger multiplicity of reaction channels.[15a] In this paper, our purpose is to qualitatively assess (on the basis of the estimate of free energy barriers), the likelihood of each of the channels, the origin and role of the vinoxyl radical, and by which pathways hydroxyl could possibly be regenerated. In the following paper (paper 2), multichannel, multiwell master equation simulations are reported and compared with the available experimental data.

Ethyne involvement is also invoked in the growth mechanism of polycyclic aromatic hydrocarbons under combustion conditions and in the chemistry of soot formation, e.g., via the HACA (*H*ydrogen *A*bstraction − C_2H_2 *A*ddition) mechanism,[15b] as well as in carbon rich stellar envelops.[16] Therefore, it would be also interesting to explore the fate of some alkynes under oxidation conditions at high temperatures. This will be the subject of a future study.[17]

Method

The study of the reaction pathways was carried out for the two alkynes by determining, on the reaction energy hypersurface, the critical points which correspond to stable and transition structures (TS). All structures were fully optimized by gradient procedures,[18] using the unrestricted Density Functional Theory (DFT),[19] with the B3LYP functional[20] and the polarized triple-ζ valence shell 6-311G(3df,2p) basis set.[21a] Some of them were reoptimized with the Dunning's cc-pVQZ basis set.[21b] The nature of the critical points was checked by diagonalization of the analytic Hessian (harmonic vibrational analysis). The doublet energies were contaminated only slightly by higher spin multiplicities in the majority of cases ($\langle S^2 \rangle \approx 0.76-0.79$). These were not corrected for spin contamination. In a few cases, in which contamination was substantial, the energies were corrected for spin contamination by the quartet, by using a formula analogous to that suggested by Yamaguchi.[22] In one case the same treatment was carried out for a contaminated singlet. The corrected stationary point energies E were then used in conjunction with the above-mentioned vibrational analysis data, to evaluate the activation and reaction enthalpies and free energies.[23] The free energy G estimates at $T = 298.15$ K will be indicated in the following as obtained "at $T = 298$ K", for short. The ΔG values (referenced to the free energies of the alkyne plus hydroxyl, denoted as **A**) are reported in the Tables 1−4 and discussed throughout the text. In some associations, the G surface was probed, looking for a possible G maximum, by drawing G profiles along an arbitrary path defined by series of constrained optimizations on the E surface, and performing the vibrational analysis by projecting out the vibrational frequency corresponding to the reaction coordinate.[24]

To obtain more reliable energetics for further use in the subsequent master equation study (paper 2), the energy difference assessments by methods such as coupled cluster, quadratic CI, or a composite method (such as CBS-QB3 or others) would be advisable (compare refs 13 and 14). However, we were able to proceed along this line only for the very first step of the

TABLE 1: ΔG^a Values for the Reaction Pathway 1a (Shown in Scheme 2 for Ethyne)

	ethyne		but-2-yne	
alkyne + HO + O_2	**A**	0.0	**a**	0.0
HO addition TS	**A−B1**	4.0	**a−b1**	3.7
hydroxyl adduct + O_2	**B1**	−27.3	**b1**	−22.5
1,3 H shift TS	**B1−C**	4.8	**b1−c**	5.7
vinoxyl radical + O_2	**C**	−57.1	**c**	−52.8
O_2 addition TS	**C−D**	−49.4	**c−d**	−46.0
peroxyl adduct	**D**	−65.6	**d**	−61.5
1,3 H shift TS	**D−J**	−24.6	**d−j**	−23.6
hydroperoxyl	**J**	−71.1	**j**	−67.3
HO loss TS	**J−cis−K**	−64.7	**j−cis−k**	−62.5
cis-dicarbonyl + HO	**cis−K**	−89.3	**cis−k**	*b*
rotational TS		−87.7		−88.2[b]
trans-dicarbonyl + HO	**trans−K**	−93.3	**trans−k**	−96.1

[a] Free energy values (at $T = 298$ K, in kcal mol^{-1}) relative to the initial reactants **A**. G is estimated from B3LYP/6-311G(3df,2p) geometry optimizations and vibrational analysis. Bold labels make reference to Schemes 2 and 3. [b] A cis minimum does not exist, because the cis geometry corresponds to a rotational TS.

TABLE 2: ΔG^a Values for the Unimolecular Pathways of the Vinoxyl Radical (Shown in Scheme 4)

vinoxyl radical	**C**	0.0
H loss TS		40.1
ketene + H		29.4
1,2 H shift TS		38.5
acetyl		−6.4
fragmentation TS		8.6
CO + CH_3		−1.5

[a] Free energy values (at $T = 298$ K, in kcal mol^{-1}). G is estimated from B3LYP/6-311G(3df,2p) geometry optimizations and vibrational analysis.

TABLE 3: ΔG^a Values for the Reaction Pathways 2a−c in Schemes 2 and 3

	ethyne		but-2-yne	
hydroxyl adduct + O_2	**B1**	−27.3	**b1**	−23.5
hydroxyl adduct + O_2	**B2**	−26.0	**b2**	−22.6
interconversion TS	**B1−B2**	−24.9	**b1−b2**	−a20.5
	Pathway 2a			
O_2 addition TS	**B1−E1**	−21.9	**b1−e1**	−17.1
cis hydroxyl peroxyl rad.	**E1**	−65.5	**(e1)**	
1,5 H shift TS	**E1−J**	−66.7	**(e1−j)**	
hydroperoxyl oxyl radical	**J**	−71.1	**j**	−68.3
HO loss TS	**J−K**	−64.7	**j−k**	−63.5
	Pathway 2b			
O_2 addition TS	**B2−E2**	−20.4	**b2−e2**	−16.3
trans hydroxyl peroxyl rad.	**E2**	−57.1	**e2**	−54.6
4-ring closure TS	**E2−F**	−29.1	**e2−f**	−25.2
Dioxetanyl radical	**F**	−42.3	**f**	−40.7
O−O bond cleavage TS	**F−G**	−37.4	**f−g**	−36.6
oxyl radical	**G**	−112.9	**g**	−108.9
β-fragmentation TS	**G−H**	−113.2	**g−h**	−110.2
carboxylic acid + acyl rad.	**H**	−136.8	**h**	−139.9
	Pathway 2c			
3-ring closure TS	**E2−L**	−35.4	**e2−l**	−35.4
alkyldioxiranyl radical	**L**	−45.7	**l**	−43.2
rearrangement TS[b]	**L−M**	−35.4	**l−m**	−31.5
hydroxyl radical ester	**M**	−127.3	**m**	−100.5
β-fragmentation TS	**M−H**	−114.3	**m−h**	−116.8

[a] Free energy values (kcal mol^{-1}) relative to the initial reactants **A** + O_2. *G* is estimated from B3LYP/6-311G(3df,2p) geometry optimizations and vibrational analysis. Capital letters make reference to Schemes 2, and lowercase letters to Scheme 3. [b] O−O bond cleavage takes place concertedly with a virtual epoxide-ring closure, but the oxyl radical epoxide never forms because the would-be epoxidic C−C bond splits in the same step, giving origin to **M**.

ethyne oxidation reaction. Then, when studying dioxygen intervention in ethyne oxidation, or equivalently the first steps in the oxidation of but-2-yne, the size of the system prevented us from proceeding any further. Furthermore, when we investigated higher level calculated results for ethyne, we found only minor changes in the relative yields of the various final products (see paper 2). Thus, to attempt (in this paper) a preliminary estimate of the branching ratios for the two chemical systems in a consistent way, we resolved to make use of the DFT-(B3LYP) results exclusively. For the first step of the ethyne oxidation (see next section), the effect of basis set enlargement has been probed at this theory level, with Dunning's correlation-consistent polarized valence quadruple-ζ (cc-pVQZ) basis set, which has 5s4p3d2f1g functions on C and O and 4s3p2d1f functions on H.[21b] Addition of diffuse functions was also explored in some calculations using the aug-cc-pVQZ basis set. Additional tests were carried out on selected reaction steps by using unrestricted DFT with different functionals, such as MPW1K[25] and KMLYP.[26] Similarly, some coupled cluster[27] energy evaluations, related to the first step of the reaction sequence, were carried out for ethyne to define a limited energy profile at the UCCSD(T)/6-311G(3df,2p), by using the geometries determined at the unrestricted B3LYP/6-311G(3df,2p) level level.

All calculations were carried out by using the GAUSSIAN03 systems of programs.[28]

Results and Discussion

The reactants, intermediates, and products are labeled by bold capital letters when making reference to the ethyne oxidation (Scheme 2), and lowercase bold letters are used for the but-2-yne reactions (Scheme 3). The same notation is used in paper 2.

SCHEME 2: Ethyne Oxidation[a]

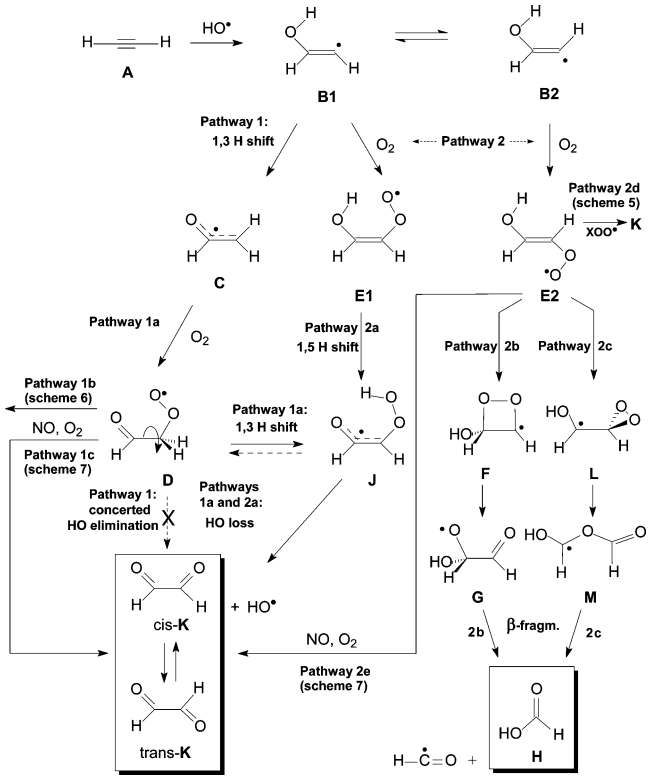

[a] Pathways **1a** (through vinoxyl, **C**) and **2a**, possibly leading to glyoxal **K**. Pathways **2b** and **2c**, potentially leading to formic acid, **H**, via hydroxydioxetanyl or hydroxydioxiranylmethyl radical intermediates, respectively. Pathway **2d** is shown in detail in Scheme 6. The NO-mediated pathways **1c** and **2e**, producing **K**, are shown in detail in Scheme 7.

The free energy differences are collected in Tables 1−6. A more complete set of total energies, enthalpies, and free energies can be found in the Supporting Information, together with the Cartesian coordinates of the critical points.

The attack by the reactive electrophilic HO radical on the triple CC bond is thought to initiate the oxidative degradation pathways.[3] When HO adds to one end of the symmetric unsaturated π system, two resulting orientations of the opposite hydrogens, or methyl groups, define the *trans* and *cis* isomers of the initial adduct, **B1** and **B2** (Scheme 2), or **b1** and **b2** for but-2-yne. The relevant free energy barrier (*G*) is estimated to be 4.0 (ethyne) or 3.7 (but-2-yne) kcal mol^{-1} higher than the *G* of the reactants, corresponding to a transition structure on the energy hypersurface. With the larger Dunning's quadruple-ζ basis set, the ethyne *G* barrier becomes 4.9 kcal mol^{-1}. The step is definitely exoergic, and the isomers have similar stability in terms of *G* (Table 1). They can also interconvert rather easily over a low barrier (Table 3).

The corresponding energy barriers are defined with respect to preceding complexes (see the Supporting Information). Complexes of this kind had been investigated theoretically by Sosa and Schlegel[29] and experimentally by Davey et al.[30] These complexes are located, for HO + ethyne, −3.5 to −3.8 kcal mol^{-1} with respect to the separate reactants (ca. −2.5 in terms of *E*+ZPE), depending on the geometric arrangement. For but-2-yne, the well is −6.9 kcal mol^{-1} deep in correspondence of the stablest arrangement (−5.3 as *E*+ZPE). Though transition structures for HO addition are found, their energy is lower than

SCHEME 3: But-2-yne Oxidation[a]

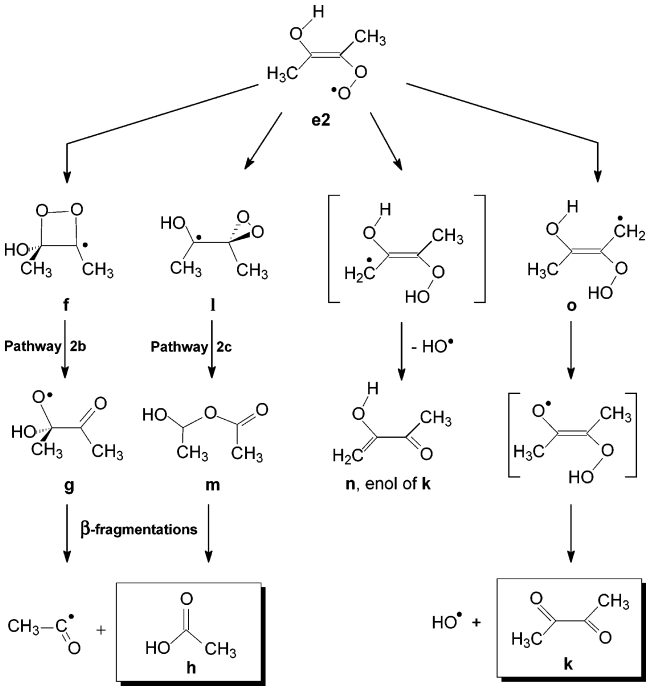

[a] Pathways **1a** (through 2-methyl-propenoxyl, **c**) and **2a**, possibly leading to dimethylglyoxal **k**, are not shown. They are identical to those sketched for ethyne in Scheme 2, apart from the nonexistence of the intermediate **e1** along pathway **2a** (center of Scheme 2). Pathways **2b** and **2c** potentially lead to acetic acid, **h**, via methyl-substituted hydroxydioxetanyl **f** or hydroxyethyldioxiranyl **l** radical intermediates, respectively. Intramolecular H-transfer pathways, followed by hydroxyl loss, can instead bring about some additional production of **k**. The NO-mediated pathways **1c** and **2e**, also producing **k**, are shown in detail in Scheme 7.

that of the reactants (−2.3 for ethyne and −4.7 for but-2-yne, as E+ZPE). The presence of a TS lower in energy than the reactants is, however, understandable because it is preceded by a complex. The negative energy barrier can also be due in part to the known inclination of B3LYP to underestimate some reaction barriers.[20] The relative energy values show at the B3LYP level a limited dependence on the basis set [6-311G-(3df,2p), −3.6; cc-pvQZ, −2.5; aug-cc-pvQZ, −2.4 kcal mol^{-1}]. We have explored the performance of two other functionals in assessing it: although MPW1K[25] gives basically a null barrier (0.01 kcal mol^{-1}), KMLYP[26] provides a negative value (−1.9 kcal mol^{-1}). A CCSD(T) estimate was then obtained by drawing an energy profile defined by a series of B3LYP geometries. These were obtained in turn by carrying out constrained optimizations at fixed inter-moiety distances. Our CCSD(T)/6311G(3df,2p) barrier height is estimated to be 1.1 kcal mol^{-1}. The comparison can be extended by taking into account results in the recent literature. SKM[13] found 1.1 kcal mol^{-1} at the RQCISD(T)/CBS level, and their B3LYP/6-311++G(d,p) datum is, not surprisingly, close to ours, −2.7 kcal mol^{-1}. On the other hand, the CBS-QCI/APNO result by Pilling and co-workers[14] is 2.6 kcal mol^{-1} (from their Figure 9a).

Regarding the stability of the initial adduct, our E+ZPE values can be compared with the MG2MS values reported by YPME in their Table 2,[12] and with the RQCISD(T)/ CBS E+ZPE values for ethyne collected by SKM in the sixth column of their Table 3,[13] and with the CBS-QCI/APNO result by Pilling and co-workers.[14] For ethyne, our −34.6 kcal mol^{-1} (**B1**) compares with the MG2MS value of −26, RQCISD(T)/CBS of −31.1 kcal mol^{-1}, and CBS-QCI/APNO of −31.2 kcal mol^{-1}.

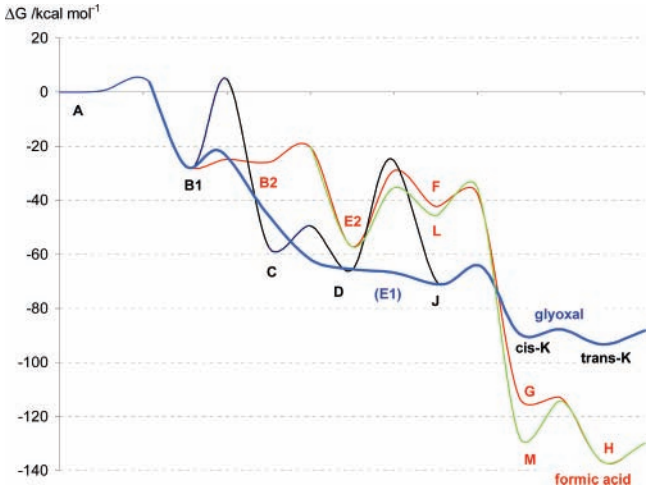

Figure 1. Ethyne oxidation. Free energy plots relevant to pathways **1a** (black), **2a** (blue), **2b** (red), and **2c** (green), estimated at T = 298 K.

For but-2-yne our −32.0 (**b1**) compares with the MG2MS value of −29 kcal mol^{-1}.

Two main series of reaction steps can then be envisaged (as illustrated for ethyne in Scheme 2) by supposing either (1) a first rearrangement step followed by dioxygen addition and subsequent HO loss (pathway **1a**; section 1) or (2) dioxygen addition followed by some monomolecular steps and a subsequent dissociation (pathways **2a**, **2b**, and **2c**). Pathway **2a** (section 2) would ultimately give way to the same product as pathway **1a**, namely a dicarbonyl compound **K** (or **k**), with concomitant HO• regeneration. In contrast, pathways **2b** and **2c** (section 3) would produce a carboxylic acid **H** (or **h**), and a carbonyl radical, which can further evolve by different channels (among which, for ethyne, HOO• production and possible HO• regeneration in the presence of NO).[3] Some intramolecular H shifts, which could take place in but-2-yne only, and give $CH_3COCOCH_3$ (**k**), are presented in section 4. The possible reaction of the key peroxyl intermediate **E2** with other peroxyl species, such as HOO•, is dealt with in section 5 for ethyne. The possible formation of H_2CO is dealt with in section 6. The picture is in fact enriched by the possible intervention of nitric oxide, which can transform any peroxyl intermediate in the schemes into the corresponding alkenyloxyl radical (pathways **1c**, branching from **D**, and **2e**, from **E**). This possibility is discussed in section 7.

1. Pathway 1a. An intramolecular 1,3 H shift in **B1** (or **b1**) causes the irreversible formation of the 2-oxoethyl (vinoxyl) radical **C**, for ethyne, or 1-methyl-2-oxopropyl (2-methyl-propenoxyl), **c**, for but-2-yne. Both have a π-delocalized electronic structure of the enolyl type (a delocalized structure which condenses the two resonance structures is displayed in Scheme 2). The stability of the **C** intermediate is assessed here as −57.1 kcal mol^{-1} with respect to the initial reactants. The relevant E+ZPE value, −64.3 kcal mol^{-1}, can be compared with the ZPE-corrected RQCISD(T)/CBS energy result by SKM (their Table 3, sixth column, and Figure 1):[13] −58.3 kcal mol^{-1}. This transformation would not be easily accessible to the system (more so for but-2-yne) as soon as the vibrationally excited adducts **B1*** or **b1*** form, because the free energy barriers for the **B1**−**C** or **b1**−**c** step are estimated to be 4.8 or 5.7 kcal mol^{-1} above the reactants **A** or **a**, i.e., slightly higher than the average energy available to the excited adduct (the barriers could be compared with those for the **A**−**B1** and **a**−**b1** steps, which are 4.0 and 3.7 kcal mol^{-1} high, respectively). The **B1**−**C** barrier

SCHEME 4: Ethyne Oxidation, Vinoxyl Rearrangement to Ketene and Vinoxyl Fragmentation via Acetyl

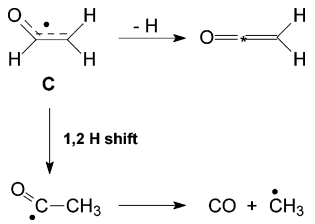

height relative to **B1** is 32.1 kcal mol^{-1} in terms of *G*, and 32.0 in terms of *E*+ZPE. This last datum can be compared with the 35.0 kcal mol^{-1} result of SKM,[13] and the 33.8 kcal mol^{-1} of Pilling and co-workers.[14]

The *G* profile for pathway **1a** (black line) is displayed in Figure 1 for ethyne. For but-2-yne it is quite similar (see the Supporting Information). A subsequent O_2 addition, with a *G* barrier of 7.6 (ethyne) or 6.8 (but-2-yne) kcal mol^{-1}, produces the peroxyl radicals **D** or **d** (in which rotation around the single C−C bond is possible). The barrier height for the **C**−**D** step was also computed at the CBS-QB3 level by Kuwata et al.[11] as 4.3 kcal mol^{-1} (in terms of *E*+ZPE), which can be compared with our *E*+ZPE difference of 2.7 kcal mol^{-1}. On the basis of the results collected by Delbos et al.[10] in their Table 4, the **C**−**D** barrier estimates (see also their Figure 10) range from 2.9 to 3.6 at the B3LYP level, to significantly higher estimates at the quadratic CI or coupled cluster leves: 6.7, 4.7 or even 12.0 kcal mol^{-1}.

Disregarding for the moment a possible role of NO (section 7), the peroxyl intermediate could in principle yield a dicarbonyl product **K** (or **k**) in two ways. One path could be a concerted HO$^{\bullet}$ elimination, the other a two-step process: an intramolecular abstraction of the geminal hydrogen to give **J** (or **j**), followed by O−O bond cleavage with HO loss. Actually, when looking for a concerted TS, a second order saddle point was found (Supporting Information), instead of a transition structure (corresponding to a first order saddle point). In the two-step process, both the *Z*- and *E*-isomers of the hydroperoxyalkenyloxyl radicals **J** and **j** can first be formed (only *Z* displayed in Scheme 2). These intermediates present the same π-delocalized radical system [O═C(R)−C$^{\bullet}$(R)O−OH ↔ $^{\bullet}$O−C(R)═C(R)O−OH] (enolyl) already encountered in the vinoxyl-type radicals (a delocalized structure which condenses the two resonance structures is displayed in Scheme 2).

Then, the O−O bond cleavage in **J** (or **j**) produces glyoxal **K** (or dimethylglyoxal **k**), and hydroxyl. For ethyne, the *trans* **K** isomer (more stable) is close in free energy to the *cis*, and the two can interconvert rather easily. In contrast, in the case of but-2-yne, the *cis* geometry of biacetyl **k** does not correspond to an energy minimum, rather it is a rotational TS. In this case, the O−O bond cleavage TS would give directly the only product, *trans*-**k** (possibly passing through the *cis*-TS dominium if HO$^{\bullet}$ loss takes place in the *Z* isomer of **j**).

Though the intermediate **C** could in principle evolve to give a dicarbonyl product, the barrier from **D** to **J** is sizable, 41 kcal mol^{-1}, as is that from **d** to **j**, 38 kcal mol^{-1}. The backward step is much easier (ca. 17 kcal mol^{-1} from **D** to **C** again, and ca. 16 kcal mol^{-1} from **d** to **c**). Because the vinoxyl-type radical **C** or **c** can hardly proceed backward to the HO−alkyne adduct, this intermediate and its dioxygen adduct could correspond to a sort of "accumulation basin", which could facilitate their detection. On the other hand, due to the high **D**−**J** barrier, it is unlikely that this pathway can contribute to dicarbonyl formation at tropospheric temperatures. However, either pathway **1b**, which leads, for ethyne, from **D** to formaldehyde and CO (see section 6), or the possible NO-mediated pathway **1c** (see section 7) could be regarded as apt to provide an escape to the reacting system from the **D**−**J** basin.

For ethyne, **C** can in principle lose one hydrogen atom to form ketene, or isomerize to form the acetyl radical, which can then decompose to produce CO + CH_3 (Scheme 4).[13,31] Ketene had indeed been observed in some experimental studies.[32] However, the free energy differences involved in these unimolecular processes (Table 2) are rather high: 40.1 kcal mol^{-1} for ketene formation and 38.5 for the isomerization to acetyl. Therefore, they could be regarded as accessible only to a nonthermalized **C** intermediate.

The relevant energy differences (corrected for ZPE) for these unimolecular steps can be compared with the *E*+ZPE values obtained at the RQCISD(T)/CBS level by SKM,[13] collected in their Figure 1 and reported here below between brackets, just following our results. A similar comparison can be drawn in part with the CBS-QCI/APNO results by Lee and Bozzelli,[31] who studied the reaction ketene + H. These will be reported in parentheses. For ketene formation we find a barrier of 40.2 kcal mol^{-1} [42.1] (43.5), and for the isomerization to acetyl of 38.3 [40.0] (40.1). Then, the ketene + H dissociation limit is located, with respect to **C**, at 35.3 kcal mol^{-1} [35.0] (35.7). The acetyl radical is at −6.0 kcal mol^{-1} [-6.8] (−5.7). Dissociation of acetyl faces then a barrier of 16.4 kcal mol^{-1} [15.7] (17.1), and the relevant CO + $CH_3^{\bullet}$ limit is at 12.1 [9.0] kcal mol^{-1} above acetyl. We compute the CBS-QCI/APNO dissociation limit as 9.9 kcal mol^{-1} above acetyl.

The relative importance of these pathways is assessed in paper 2: there it is shown that the nonthermalized **C** preferentially and rather efficiently follows the unimolecular pathways to ketene or acetyl, rather than evolving to **D**. In the end, this finding appears to be in accord with the unsuccessful experimental attempt to detect a vinoxyl radical reported by YPME.[12]

Regarding the but-2-yne system, paper 2 shows that that a more efficient thermalization of **b1** even prevents a significant formation of **c**.

2. Pathway 2a. Pathway **2**, upon O_2 addition to the either **B1** (**b1**) or **B2** (**b2**), splits right from the beginning into pathways **2a** and **2b**. For ethyne, this corresponds to the formation of the peroxyl radical isomers **E1** and **E2** (the *G* profile for pathway **2a**, in blue, is displayed in Figure 1). However, in the case of but-2-yne, the energy minimum corresponding to **e1** is not detectable on the hypersurface, because, as dioxygen adds, the hydroxyl group very easily loses its hydrogen, which gets bound to the terminal peroxyl oxygen (O′). Because the **e1** minimum is not present, the only end result of such a geometry optimization is the hydroperoxylalkenyloxyl radical intermediate **j**. Indeed, no O_2 addition TS is found on either the ethyne or the but-2-yne energy hypersurfaces, but only a descending path, down from **B1** (or **b1**), which leads, in the case of ethyne, to **E1**, or, in the case of but-2-yne, to **j**. These results are consistent with the fact that a hydroxyperoxyl radical such as **E** was not reported in the study by YPME.[12]

In the case of but-2-yne, we attempted to get a clearer picture of the concerted nature of this process of dioxygen addition and H transfer. For this purpose, a series of constrained optimizations were carried out for the but-2-yne system, with the O−C distance held fixed at 3.1, 3.0, ..., down to 1.36 Å (for details, see the Supporting Information). All points so defined present the original O−H bond either unmodified with respect to **b1**, where O−H = 0.963 Å, or barely stretched at shorter O−C distances (e.g., at O−C = 1.5 Å, where O−H =

0.993 Å). Meanwhile, some interaction of the hydroxyl H with the O′ atom of the incoming dioxygen builds up, as indicated by H−O′ distances as short as 1.617 Å at O−C = 1.5 Å. When the O−C distance of 1.38 Å is reached, the O−H stretches more significantly to 1.028 Å, then, at O−C = 1.36 Å, the hydrogen jumps abruptly onto the terminal peroxyl oxygen O′.

A first feature in terms of free energy is that a maximum along the *G* profile is found for both alkynes. It occurs at O−C = 2.1 (ethyne, barrier of 5.4 kcal mol^{-1}) or 2.2 Å (but-2-yne, barrier of 6.4 kcal mol^{-1}), so rather early, in a geometrical sense, if the structural traits just discussed are considered. In fact, the second event, the H transfer, takes place well beyond this maximum (of course, the description in terms of free energy cannot be but very approximate). At any rate, the overall process leading from **B1** (or **b1**) to **J** (or **j**) can be seen as concerted, yet highly asynchronous. A second attribute of the *G* profile is that the **E1** depression disappears even for ethyne. Although pathway **2a** passes through a 1,5 H shift TS to produce **J**, this process is described as barrierless in terms of *G*.

Because **J** can undergo O−O bond cleavage and HO loss with a *G* barrier of only 4.8 (ethyne), and **j** with a *G* barrier of 6.4 (but-2-yne) kcal mol^{-1}, pathway **2a** ultimately gives *cis*-(and then *trans*-)glyoxal **K** (ethyne) or *trans*-dimethylglyoxal **k** (but-2-yne) with concurrent HO regeneration.

The energies (corrected for ZPE) of our **E1** and **J** intermediates can be compared again with those reported by YPME in their Table 2.[12] **E1** is located (for ethyne) at −83.3 kcal mol^{-1} (**E2** at −73.5) with respect to the initial reactants, to be compared with a single MG2MS value of −74 kcal mol^{-1} (relevant to the *cis* isomer). **J** is found, for ethyne, at −88.7 kcal mol^{-1}, and for but-2-yne **j** is at −86.7 kcal mol^{-1}. These values compare with the MG2MS values of −81 and −84 kcal mol^{-1}, respectively.

Regarding the final dicarbonyl products, our values for ethyne are −97.3 (*cis*-**K**) and −101.6 (*trans*-**K**) kcal mol^{-1}, to be compared with −104 kcal mol^{-1} at the MG2MS level. For but-2-yne, *trans*-**k** is at −112.0 kcal mol^{-1}, and the MG2MS value (for the trans isomer) is −112 kcal mol^{-1}.

Thus, pathways **1a** and **2a** merge in correspondence of the *Z*-**J** (or *Z*-**j**) isomer (though both **D** and **d** can rotate and give also *E*-**J**), and finally converge on the same dicarbonyl products. Pathway **2a** appears to offer a much easier route (Tables 1 and 2). HO$^{\bullet}$ is regenerated through both pathways, but in the ethyne reacting system its hydrogen is certainly the original hydroxyl hydrogen only for pathway **2a** (in **D** the choice is between two equivalent methylenic hydrogens). For the but-2-yne reacting system, the hydrogen belonging to the regenerated HO$^{\bullet}$ would obviously come from the original hydroxyl radical. These points can be taken by inspecting Schemes 2 and 3. These results are in contrast with the reported DO$^{\bullet}$ detection in the reaction HO$^{\bullet}$ + C_2D_2, carried out as described in ref 5, because this DO$^{\bullet}$ cannot be the outcome of pathway **2a**. In contrast, following pathway **1a**, it can be seen that for ethyne the hydrogen abstracted in the step **D**−**J**, and becoming the hydroxyl hydrogen, could as well come from the original alkyne. In the case of but-2-yne, the only available hydrogen would be in any case that coming from the reactant hydroxyl, along both **1a** and **2a** pathways. However, it seems unlikely that the regenerated HO$^{\bullet}$ comes from pathway **1a**, for both alkynes.

3. Pathways 2b and 2c. A different outcome is opened by pathway **2b**, which corresponds to the scheme proposed in ref 5 (eq 23, p 177) or in ref 3 (eq 3, p 2079).

The corresponding *G* profile, in red, is shown in Figure 1. Once dioxygen had added to **B2**, ring closure in **E2** can lead to a dioxetanyl radical **F** (Scheme 2, right, pathway **2b**). Ring closure is the key step for obtaining in the end a carboxylic acid, because one carbon gets bound to two oxygen atoms. However, the barrier height for step **E2**−**F** is significant, and this evolution seems viable only if one assumes that at least some nonthermalized adduct **E2** is present (these aspects are addressed more fully in paper 2). Then, the peroxy bond cleavage in **F** produces the oxyl radical intermediate **G**. Finally, **G** undergoes the β-fragmentation that yields a carboxylic acid plus a carbonyl radical. The overall pathway is significantly more exoergic than those leading to the dicarbonyl products (Figure 1). Yet, the height of the **E2**−**F** barrier could limit its importance severely, if the greater part of the **E2** which forms gets thermalized.

Regarding carboxylic acid formation, YPME (ref 12, p 1884) interestingly recalled a suggestion put forward by Carpenter[33] in a theoretical mechanistic study on the reaction of dioxygen with the vinyl radical, concerning the intervention of a dioxiranylmethyl radical intermediate. Thus, YPME in turn suggested that in alkyne oxidation a dioxirane-ring containing intermediate could play an important role in the formation of the carboxylic acids. Their suggestion relies on the energy of the intermediate itself, which came out to be lower than that of the dioxetane-like intermediate.[12]

We have explored the entire reaction pathway which could originate from this different ring closure mode in **E2** (Scheme 2, right, pathway **2c**). O−O bond cleavage in the alkyl dioxiranyl radical intermediate **L** would presumably give way, through spin recoupling, to the formation of an epoxidic ring in a hydroxyl oxyl radical intermediate. A species with this structure could not be found, because the epoxidic ring closure through C−O bond formation takes place concertedly with C−C bond cleavage in the same "latent ring" (as sketched below, curled arrows), to produce an ester functionality in the intermediate which directly follows **L**, the radical **M** (compare Scheme 2). Then **M**, upon β-fragmentation, produces the carboxylic acid **H** and the R−C═O radical. The free energy profile for pathway **2c** (depicted in Figure 1, in green), is rather close to that of pathway **2b**.

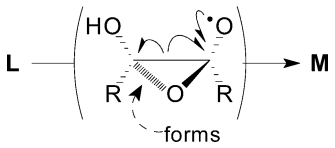

The stability in terms of *E*+ZPE values found here for the dioxetanyl and dioxiranyl radical intermediates can be compared again with the MG2MS results of YPME.[12] **F** and **L** (ethyne system) are −60.2 and −63.0 kcal mol^{-1} below the reactants (−57 and −59 kcal mol^{-1} at the MG2MS level); **f** and **l** (but-2-yne system) are located here at −60.4 and −63.0 kcal mol^{-1}, and the MG2MS estimates are −62 and −70 kcal mol^{-1}, respectively. The final products are at −143.6 kcal mol^{-1} (**H**, for the ethyne system) and −146.8 (**h**, for the but-2-yne system). The corresponding MG2MS values are: −136 and −145 kcal mol^{-1}, respectively.

The formation of the H−C═O radical in the last step opens (for ethyne only) a hydroxyl regeneration channel alternative to the HO loss step **J**−**K** of pathway **2a**. This could be mediated by O_2 (to give HOO$^{\bullet}$ + CO) and finally by NO (through HOO$^{\bullet}$ → HO$^{\bullet}$). If the initial ethyne were DC≡CD, the radical would be D−C═O (compare Scheme 2) and would ultimately generate DO$^{\bullet}$ via DOO$^{\bullet}$. If, on the other hand, a deuterated hydroxyl were used to react with ethyne (as done in ref 6), HCOOD would

SCHEME 5: Pathway 2d for Ethyne, Reaction of E2 with a Peroxyl Species

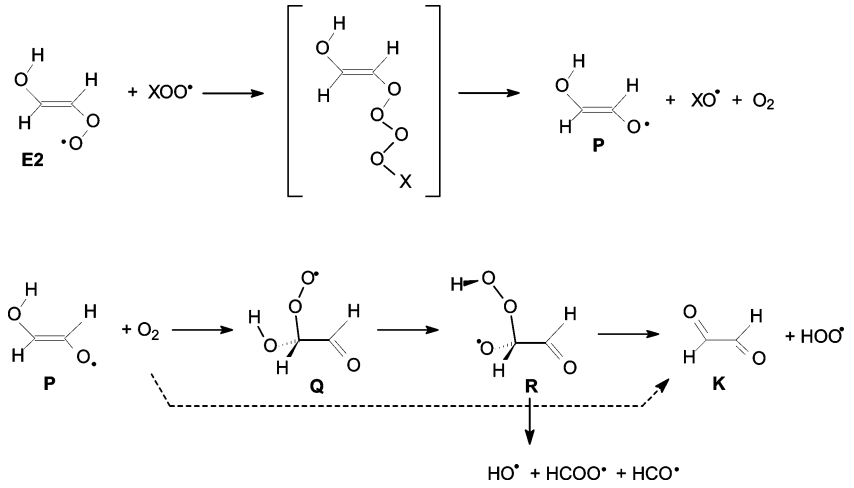

form, and normal glyoxal plus regenerated DO• by pathway **2a**, as the terminal O in **J** would abstract the original hydroxyl D.

The relevant free energy profiles are qualitatively and quantitatively similar for the two alkynes, though *cis*-K is an energy minimum only for ethyne (see Figure A in the Supporting Information). The only differences are along the energy profiles, where **e1** does not exist as an energy minimum for but-2-yne, but for ethyne it does.

In the absence of NO, at room temperature, pathway **2a** is preferred. Though pathway **1a** is not competitive, the vinoxyl radical **C** had been detected by LIF in a study on ethyne oxidation by hydroxyl and dioxygen.[5] Independent studies on **C**, generated by photolysis of methyl vinyl ether,[8,9,10] in which delayed formation of glyoxal was observed (9×10^{-4} s) - with respect to the disappearance of the vinoxyl radical (9×10^{-5} s), suggested that **C** can give a long-lived adduct with O_2.[8] This is qualitatively consistent with our calculations, which suggest a not very easy (if the adduct **B1** is supposed to be available as a mostly thermalized species) but irreversible formation of **C**, along with its possible accumulation, to some extent, in equilibrium with its dioxygen adduct **D**, which faces in turn a difficult step toward the products (Figure 1).

These results qualitatively suggest a prevailing yield of dicarbonyl product, larger than 90%, for both alkynes (in ref 6 a 70 ± 30% yield was experimentally determined for ethyne, and 87 ± 7% for but-2-yne). In paper 2 the theoretical yields are assessed in more detail by using master equation simulations.

The computational results point out the limited importance of channel **1a** in producing the dicarbonyl compounds when the starting point is the alkyne. But this is of course the only channel available in the methyl vinyl ether photolysis studies,[9,10] in which a much lower yield is found. The present results offer an explanation for the higher yield observed in the experimental investigations on alkyne oxidation, because the more efficient channel 2a is in that case accessible. As already mentioned, it is shown in paper 2 that a non thermalized **C** will follow the unimolecular pathways to ketene or acetyl, rather than evolving to **D**.

4. Intramolecular H Shifts in the But-2-yne Reacting System. Two further intramolecular reactions are possible in but-2-yne only. They could start from **e2** and provide in principle carbonyl products (Scheme 3, right). The reactions begin with a hydrogen transfer in **e2** from one methyl group to the terminal oxygen. In one case this abstraction comes out to be concerted with hydroxyl loss, and brings about the formation of **n**, the enol of **k**. The free energy barrier in going from **e2** to **n** is 25.5 kcal mol^{-1} high; **n** is in turn located at −28.8 kcal mol^{-1} with respect to **e2** (−82.3 with respect to **a** + HO•). From this species, however, the tautomerism to the keto form (**k**) requires, as expected for a gas-phase process, a high-energy barrier (53.1 kcal mol^{-1} with respect to **n**). In the other case, the allyl radical system **o** forms (with a barrier from **e2** of 27.3 kcal mol^{-1}); **o** is located at 4.7 kcal mol^{-1} above **e2** (−48.8 with respect to **a** + HO•). Then **o** undergoes another H transfer (from the OH group to the radical C center) concerted with HO• loss, and gives **k**, with a barrier of 24.6 with respect to **o**).

TABLE 4: ΔG^a Values for the Reaction Pathway 2d (Studied for Ethyne Only) Leading from E2 + HOO• to K

peroxyl radical	**E2**	0.0
hydroxy oxyl radical + $^3O_2$	**P**	−33.7
hydroxy oxyl radical	**P**	0.0
O_2 addition TS	**P**−**Q**	9.3
hydroxy peroxyl radical	**Q**	−2.9
1,4 H shift TS	**Q**−**R**	8.5
hydroperoxyl oxyl radical	**R**	6.7
HOO loss TS	**R**−**K**	8.5
trans hydroxyl peroxyl radical	**K**	−0.7

[a] Free energy values (kcal mol^{-1}). *G* is estimated from B3LYP/6-311G(3df,2p) geometry optimizations and vibrational analysis. Capital letters make reference to Scheme 5.

5. Pathway 2d (Ethyne System): Reaction with a Peroxyl Species. **E2** could also react with another **E2** molecule (self-reaction) or more likely with HOO (or ROO) radicals (cross reactions) to form the oxyl-hydroxyl radical **P** (pathway **2d**, Scheme 5, and Table 4). Typical (collective) concentrations of these radicals are reported in ref 3 to be as high as 12−13 ppt (Chapter 6.2, pp 238, 239) or, consistently, 10^8−10^9 molecules cm^{-3} (Chapter 11.4, pp 606, 607). The reactions with XOO• species are most likely to occur when **E2** is completely thermalized (see paper 2: Table 2 in the section "ethyne + OH reaction" and Table 3 in the section "but-2-yne + OH reaction"). There it is shown that thermalized **E2** can represent up to 0.4% of the reacted ethyne. Similarly, **e2** could be up to 7.5% of the reacted but-2-yne, but the study was not extended to it because **e2** completely reacts before thermalization (see paper 2). The rate of these bimolecular reactions would obviously be slow because of the low concentration of reactants, but glyoxal would be obtained easily. The reaction of **E2** is highly exoergic ($\Delta G_{E2-P} = -75.2$ kcal mol^{-1}). From **P**, O_2 can extract the hydroxyl H to produce glyoxal **K**. This could in principle be a direct H abstraction which gives **K** (dashed arrow in Scheme 5). However, this TS cannot be found and the resulting pathway consists of three steps: O_2 addition (giving the intermediate

SCHEME 6: Unimolecular Steps for the Ethyne System, Apt to Lead, in Principle, to Formaldehyde Production[a]

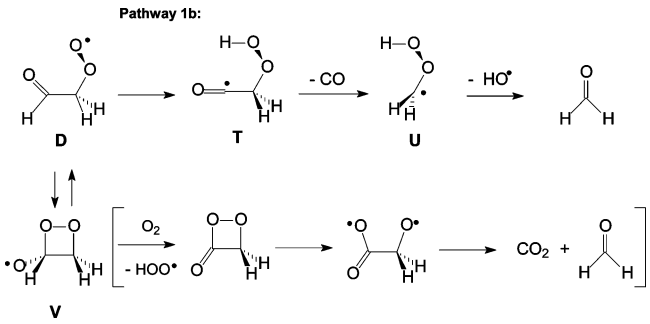

[a] Paper 2 indicates that the importance of the pathway going through **V** is very low.

TABLE 5: ΔG^a Values for the Reaction Pathway 1b Producing Formaldehyde

1,5 H shift TS	**D**−**T**	−44.9
hydroperoxy acyl radical	**T**	−61.4
CO loss TS	**T**−**U**	−52.8
hydroperoxymethyl rad. + CO	**U**	−65.2
formaldehyde + CO + HO•		−103.3

[a] Free energy *G* values (kcal mol^{-1}) relative to the initial reactants **A** + HO• + O_2. *G* is estimated from B3LYP/6-311G(3df,2p) geometry optimizations and vibrational analysis. Capital letters make reference to Scheme 6.

Q), hydrogen transfer (to get **R**) and finally HOO• loss (yielding **K** again). The step from **R** indicated by a downward arrow in the scheme is not competitive, because the dissociation limit for HO + HCOO + HCO is ca. 20 kcal mol^{-1} above that for **P**.

6. Formaldehyde Formation: Pathway 1b. Formaldehyde was not detected in the experimental study on ethyne oxidation of ref 6. However, a decomposition pathway giving formaldehyde was suggested (on p 3905) in the paper by Gutman and Nelson.[9] A formaldehyde-producing channel was also suggested by Zhu and Johnston.[8] Also Delbos et al.[10] and Kuwata et al.[11] considered this possibility (eqs 2−4 in ref 10; eqs 15 and 24 in ref 11) and their results can be compared with ours.

Some pathways apt to produce formaldehyde have been considered here for ethyne only (Scheme 6, in which some steps are not accessible to but-2-yne). Stemming from **D**, the dioxygen adduct to the vinoxyl radical, the two steps to **T** or **V** have been found to require 20.7 or 28.9 kcal mol^{-1}, respectively ($\Delta G^{\ddagger}$ at $T = 298$ K). We can now compare our E+ZPE **D**−**T** barrier (19.8 kcal mol^{-1}) with (i) those computed for the vinoxyl system by Delbos et al.[10] (20.2−20.4 kcal mol^{-1} at the B3LYP level, or 22.5−23.3 kcal mol^{-1} at the coupled cluster and quadratic CI levels; see Table 4 in ref 10), and (ii) with the value assessed by Kuwata et al.[11] at the CBS-QB3 level, which is 19.5 kcal mol^{-1}.

The more viable pathway has been defined, as shown in Scheme 6, by determining the structures of the intermediates **T** and **U**, as well as the transition structures connecting them, which define pathway **1b**. A free energy descent is found, in which the last step (formaldehyde formation with CO loss), has a tiny energy barrier but presents no barrier at all in terms of free energy. Our E+ZPE **T**−**U** barrier height is 13.2 kcal mol^{-1}, and that computed at the CBS-QB3 level is 11.4 kcal mol^{-1}.[11] The braching ratio depends on the two barriers: for the **D**−**T** step the barrier height is 20.7 kcal mol^{-1} and for the for the **D**−**J** step is 41.0 kcal mol^{-1}. We can recall that also Kuwata et al.[11] assess the **D**−**J** CBS-QB3 barrier height at 39.1 kcal mol^{-1} (E+ZPE), which is comparable to our E+ZPE barrier of 40.6 kcal mol^{-1}. If NO is absent, one can conclude that all **D** that forms is subsequently converted to formaldehyde. However, because the NO-mediated pathway **1c** is more viable (see section 7), in the case of thermalized **D**, its can suppress formaldehyde formation altogether.

On the other hand, the pathway that originates from **V** is conceivable but cannot be competitive, because of the higher **D**−**V** barrier (see paper 2). For this reason, it will not be discussed any further here.

SCHEME 7: Pathways Involving NO Intervention[a]

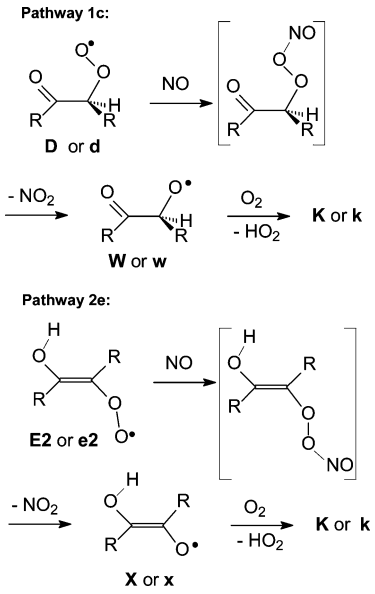

[a] R stays for hydrogen (ethyne, uppercase labels) or methyl (but-2-yne, lowercase labels). HO_2, in the presence of NO, can be source of HO.

TABLE 6: ΔG^a Values for the NO-Mediated Reaction Pathways 1c and 2e

	ethyne		but-2-yne	
Pathway 1c				
peroxyl adduct + NO + O_2	**D**	−65.6	**d**	−61.5
peroxynitrite adduct + O_2		−74.2		−70.0
oxyl precursor of K + O_2	**W**	−84.4	**w**	−82.1
H abstraction TS by O_2		−72.2		−70.5
cis−dicarbonyl + HOO•	**K**	−103.8	**k**	*−102.7*[b]
trans−dicarbonyl + HOO•	**K**	−107.8	**k**	−110.6
Pathway 2e				
peroxyl adduct + NO + O_2	**E2**	−57.1	**e2**	−53.5
peroxynitrite adduct + O_2		−66.5		−61.4
oxyl precursor of *trans*-K + O_2	**X**	−105.8	**x**	−101.9
H abstraction TS by O_2		−85.0		−92.8

[a] Free energy *G* values (kcal mol^{-1}) relative to the initial reactants **A** + HO• + O_2 + NO + O_2 for pathway **1c** and **2e**. *G* is estimated from B3LYP/6-311G(3df,2p) geometry optimizations and vibrational analysis. Capital letters make reference to Scheme 7. [b] A cis minimum does not exist, because the cis geometry corresponds to a rotational TS.

7. NO Intervention: Pathways 1c and 2e. Nitric oxide can extract the terminal oxygen of any peroxyl radical intermediate. We will neglect the minor channel that leads to organic nitrates. Considering the **E** (**e**) adducts, because the intramolecular transformation to **J** (**j**) is quite easy, and **e1** is not detected on the *G* surface, the NO-mediated pathway has been studied only for **E2** and **e2**. The transformations **D**−**W**−**K** (pathway **1c**) and **E2**−**X**−**K** (pathway **2e**), only hinted at in Schemes 2 and 3, are shown in more detail in Scheme 7. Though peroxynitrite adducts (between brackets) are found on the energy hypersurface

(see the Supporting Information), their importance is likely to be very small in terms of free energy (Table 6). Upon reaction of NO with **D** or **E2**, two irreversible free energy cascades are found, leading to the oxyl intermediates **W** or **X** and then to the dicarbonyl products. In the ethyne system the free energy barrier for the step **E2**−**L** is 21.7 kcal mol^{-1} (27.9 for **E2**−**F**). For the similar **e2**−**l** step in the but-2-yne system it is 19.2 kcal mol^{-1} (29.4 for **e2**−**f**). Therefore, if the **E2** or **e2** intermediates were able to thermalize efficiently, the exceedingly easy NO-mediated process would appear as prevailing completely at any reasonable NO concentration, which can be considered as ranging from 10^8 molecules cm^{-3}, representative of an unpolluted situation, to 10^{14} molecules cm^{-3} (a typical value in the engine exhaust, but peak values can be higher).[34] This is of course true only if the **E2** or **e2** intermediates are thermalized; otherwise the unimolecular step would prevail, because the bimolecular reaction is slower than thermalization. It is clear at this point that whether pathway **2e** is actually apt to increase to some extent the dicarbonyl compound yield, and concurrently decrease the acid yield, can be assessed only by the approach followed in paper 2.

Similarly, if NO is present, pathway **1c** could be largely dominant over any other possibility stemming from **D**. Accordingly, all the available **D** could become a source of regenerated HO or DO radicals. However, it will be seen in paper 2 that the amount of **C** formed is very small (even smaller than the yield of **D**).

If the NO-mediated pathway happens to be actually dominant, only the dicarbonyl product should form. This conclusion (based on the hypothesis of thermalized intermediates) would be in disagreement with the results of Hatakeyama, Washida and Akimoto,[6] regarding the ethyne system. They did not find in fact any change in the carboxylic acid to dicarbonyl product ratio upon addition of NO up to 6 mtorr (compare ref 6, p 176). Therefore, their result could suggest a very short lifetime for a possibly nonthermalized **E2**, which would prefer to undergo the intramolecular step to **L** (or **F**). In fact, paper 2 indicates that a very minor fraction of **E2** attains thermalization.

Concluding Remarks

From the results of the hypersurface probing and the free energy differences so assessed, we can only draw preliminary and qualitative conclusions about the feasibility of the reaction pathways detected. A more detailed analysis is reported in paper 2. The main findings of paper 1 are the following.

The first step in the symmetric alkyne oxidations studied is the formation of two equilibrating hydroxyl adducts, **B1** and **B2** for ethyne, or **b1** and **b2** for but-2-yne. From these, several pathways depart.

(1) Pathway **1a**, to the vinoxyl-type radical **C** (or **c**) via a H-shift taking place in the initial HO-alkyne adduct. This rearrangement does not appear to be easily accessible to the system (more so for but-2-yne) because the free energy barriers are slightly higher than the average energy available to the excited adducts. In paper 2 it is shown that most of the **C** formed does not attain thermal equilibrium and evolves instead through unimolecular steps to ketene, or to CO and $CH_3^{\bullet}$, whereas **c** does not form in a significant amount. Ketene has indeed been observed in experimental studies.[32]

(2) For pathway **1b**, the vinoxyl-type intermediate and its dioxygen adduct, a peroxyl radical, are described as defining a free energy "basin", which could be populated if vinoxyl itself were thermalized. The escape from the basin could then occur in that case through a unimolecular process which leads to formaldehyde. Formaldehyde was not detected in the study of ref 6 (p 175), but it was observed in ref 8, starting from vinoxyl. It can be concluded that the two pathways involving a vinoxyl-type intermediate do not represent an efficient route to dicarbonyl compound formation.

(3) For pathway **1c**, if NO is present, the population of the dioxygen adduct of the vinoxyl-type radical (a peroxyl intermediate) can be depleted via reaction with NO, which brings about again the formation of a dicarbonyl compound. In that case, all the available **D** could become a source of regenerated hydroxyl radicals. This can, however, hardly compete with the unimolecular pathway to formaldehyde.

(4) Pathway **2a**, initiated by dioxygen addition to the **B*n*** or **b*n*** intermediates, goes down a steep free energy profile leading to dicarbonyl **K** (or **k**) formation and concomitant HO$^{\bullet}$ production. It is the most promising pathway toward the main products. It regenerates HO$^{\bullet}$. Both these findings are consistent with the experimental results, which indicate the dicarbonyl compounds as major products,[6] accompanied by hydroxyl regeneration.[5,7]

(5) Pathways **2b** and **2c** are characterized by different unimolecular transformations of the *E*-peroxyl adducts **E2** (or **e2**). These pathways lead either to dioxetanyl **F** or **f** (**2b**) or to alkyldioxiranyl **L** or **l** (**2c**) cyclic radicals. Then, through their intermediacy, these pathways could end up producing a R−C═O radical plus a carboxylic acid, **H** or **h** (the second major product), via successive O−O bond cleavages and β-fragmentations. These pathways are not as facile as **2a** but could be viable to some extent (in particular pathway **2c**), in qualitative agreement with the experimental results, which indicate carboxylic acids as the second major products.[6]

(6) For but-2-yne only, some intramolecular H shifts open a possible extra channel for dicarbonyl product formation.

(7) Pathway **2d**, by which the peroxyl adduct **E2** can react with another peroxyl compound, opens a different pathway to **K**. Though apparently promising, the rate of this process is expected to be much slower than the unimolecular channels, due to the low concentrations of the reactants.

(8) Pathway **2e**. Another NO-mediated process could divert the thermalized peroxyl adducts **E2** or **e2** from pathways **2b** and **2c** and consequently depress carboxylic acid (**H**) formation in favor of some enhancement of dicarbonyl compound (**K**) formation. Also this NO-mediated pathway can be identified as a source of hydroxyl. However, as will be seen in paper 2, **E2** is thermalized to a small extent, in such a way that NO can hardly affect the carboxylic acid to dicarbonyl product ratio. This is in accord with the experimental findings of ref 6, in which no significant changes in product ratios were observed upon addition of ca. 10^{14} molecules cm^{-3} of NO.

Acknowledgment. This work had financial support by the Italian MIUR within the PRIN-COFIN 2004 "Studio integrato sul territorio nazionale per la caratterizzazione ed il controllo di inquinanti atmosferici (SITECOS)". It was conducted in the frame of EC FP6 NoE ACCENT (Atmospheric Composition Change, the European NeTwork of Excellence).

Supporting Information Available: Cartesian coordinates (txt file), energies, enthalpies, and free energies of the critical points. This information is available free of charge via the Internet at http://pubs.acs.org.

References and Notes

(1) See for instance: Greenberg, J. P.; Zimmermann, P. R. *J. Geophys. Res.* **1984**, *89*, 4767.

(2) Wayne, R. P. *Chemistry of Atmospheres*; Clarendon Press: Oxford, U.K., 1996; pp 252−263.

(3) Finlayson-Pitts, B. J.; Pitts, J. N., Jr. *Chemistry of the Upper and Lower Atmosphere*; Academic Press: New York, 2000; Chapter 6.

(4) Boodaghians, R. B.; Hall, I. W.; Toby, F. S.; Wayne, R. P. *J. Chem. Soc., Faraday Trans. 2* **1987**, *83*, 2073.

(5) Schmidt, V.; Zhu, G. Y.; Becker, K. H.; Fimk, E. H. *Ber. Bunsen-Ges. Phys. Chem.* **1985**, *89*, 321.

(6) Hatakeyama, S.; Washida, N.; Akimoto, H. *J. Phys. Chem.* **1986**, *90*, 173.

(7) Bohn, B.; Zetzsch, C. *J. Chem. Soc., Faraday Trans.* **1998**, *94*, 1203. Bohn, B.; Siese, M.; Zetzsch, C. *J. Chem. Soc., Faraday Trans.* **1996**, *92*, 1459−1466. Siese, M.; Zetzsch, C. *Z. Phys. Chem.* **1995**, *188*, 75. Zetzsch, C.; Koch, R.; Bohn, B.; Knispel, R.; Siese, M.; Witte, F. "Adduct Formation of OH with Aromatics and Unsaturated Hydrocarbons and Consecutive Reactions with O_2 and NO_x to Regenerate OH". In *Transport and Chemical Transformation of Pollutants in the Troposphere*; Le Bras, G., Ed.; Chemical Processes in Atmospheric Oxidation, Vol. 3; Spinger Verlag: Berlin, 1995; Chapter 3.25.

(8) Zhu, L.; Johnston, G. *J. Phys. Chem.* **1995**, *99*, 15114.

(9) Gutman, D.; Nelson, H. H. *J. Phys. Chem.* **1983**, *87*, 3902.

(10) Delbos, E.; Fittschen, C.; Hippler, H.; Krasteva, N.; Olzmann, M.; Viskolcz, B. *J. Phys. Chem. A* **2006**, *110*, 3238−3245.

(11) Kuwata, K. T.; Hasson, A. S.; Dickinson, R. V.; Petersen, E. B.; Valin, L. C. *J. Phys. Chem. A* **2005**, *109*, 2514−2524.

(12) Yeung, L. Y.; Pennino, M. J.; Miller, A. M.; Elrod, M. J. *J. Phys. Chem. A* **2005**, *109*, 1879−1899.

(13) Senosiain, J. P.; Klippenstein, S. J.; Miller, J. A. *J. Phys. Chem. A* **2005**, *109*, 6045−6055.

(14) McKee, K. W.; Blitz, M. A.; Cleary, P. A.; Glowacki, D. R.; Pilling, M. J.; Seakins, P. W.; Wang, L. *J. Phys. Chem. A* **2007**, *111*, 4043−4055.

(15) (a) Part of this work was presented at the ACCENT Symposium "The Changing Chemical Climate of the Atmosphere" held in Urbino, Italy, September 2005. (b) Bittner, J. D.; Howard, J. B. *Proc. Combust. Inst.* **1981**, *18*, 1105. Bockhorn, H.; Fetting, F.; Wenz, H. W. *Ber. Bunsen-Ges. Phys. Chem.* **1983**, *97*, 1067. Frenklach, M.; Clary, D. W.; Gardiner, W. C.; Stein, S. E. *Proc. Combust. Inst.* **1984**, *20*, 887.

(16) Cherchneff, I.; Barker, J. R.; Tielens, A. G. G. M. *Astrophys. J.* **1992**, *401*, 269−287. *Ibidem* **1993**, *413*, 445−445.

(17) Tonachini, G.; Giordana, A.; Indarto A. "PAH growth through the HACA mechanism in a model unsaturated hydrocarbon radical/ethyne system adsorbed on a soot platelet. A theoretical study", 41th IUPAC Congress "Chemistry Protecting Health, Natural Environment, and Cultural Heritage", Torino, Italy, August 2007.

(18) Pople, J. A.; Gill, P. M. W.; Johnson, B. G. *Chem. Phys. Lett.* **1992**, *199*, 557. Schlegel, H. B. In *Computational Theoretical Organic Chemistry*; Csizsmadia, I. G., Daudel, Eds.; Reidel Publishing Co.: Dordrecht, The Netherlands, 1981; pp 129−159. Schlegel, H. B. *J. Chem. Phys.* **1982**, *77*, 3676. Schlegel, H. B.; Binkley, J. S.; Pople, J. A. *J. Chem. Phys.* **1984**, *80*, 1976. Schlegel, H. B. *J. Comput. Chem.* **1982**, *3*, 214.

(19) (a) Parr, R. G.; Yang, W. *Density Functional Theory of Atoms and Molecules*; Oxford University Press: New York, 1989; Chapter 3. (b) Jensen, F. *Introduction to Computational Chemistry*; John Wiley: New York, 1999. (c) Koch, W.; Holthausen, M. C. *A Chemist's Guide to Density Functional Theory*; John Wiley: New York, 2000.

(20) B3: Becke, A. D. *Phys. Rev. A* **1988**, *38*, 3098. Becke, A. D. *ACS Symp. Ser.* **1989**, *394*, 165. Becke, A. D. *J. Chem. Phys.* **1993**, *98*, 5648. (b) LYP: Lee, C.; Yang, W.; Parr, R. G. *Phys. Rev. B* **1988**, *37*, 785. This approach is based on the popular functional B3LYP, which has encountered widespread success because of its rather satisfactory performances (see for instance ref 18b, p 189, and ref 18c, pp 82 and 141). However, it is known to be inclined to underestimate some barriers, specifically for H-transfer reactions. Other functionals have been proposed (see for instance refs 25 and 26) in an attempt to address this problem. In particular, the work by Truhlar's group can be mentioned (see: http://comp.chem. umn.edu/info/DFT.htm; Zhao, Y.; Truhlar, D. G. *Theor. Chem. Acc.* **2007**, available online at http://dx.doi.org/10.1007/s00214-007-0310-x).

(21) (a) Hehre, W. J.; Ditchfield, R.; Pople, J. A. *J. Chem. Phys.* **1972**, *56*, 2257. Hariharan, P. C.; Pople, J. A. *Theor. Chim. Acta* **1973**, *28*, 213. Frisch, M. J.; Pople, J. A.; Binkley, J. S. *J. Chem. Phys.* **1984**, *80*, 3265. (b) Dunning, T. H., Jr. *J. Chem. Phys.* **1989**, *90*, 1007.

(22) Yamanaka, S.; Kawakami, T.; Nagao, K.; Yamaguchi, K. *Chem. Phys. Lett.* **1994**, *231*, 25. Yamaguchi, K.; Jensen, F.; Dorigo, A.; Houk, K. N. *Chem. Phys. Lett.* **1988**, *149*, 537. See also: Baker, J.; Scheiner, A.; Andzelm, J. *Chem. Phys. Lett.* **1993**, *216*, 380. For discussions concerning the effect of spin projection on the performances of DFT methods, see: Wittbrodt, J. M.; Schlegel, H. B. *J. Chem. Phys.* **1996**, *105*, 6574 (where some drawbacks of the projection procedures are discussed, which can suggest not to use them). Goldstein, E.; Beno, B.; Houk, K. N. *J. Am. Chem. Soc.* **1996**, *118*, 6036.

(23) Reaction enthalpies and entropies were computed as outlined, for instance, in: Foresman, J. B.; Frisch, Æ. *Exploring Chemistry with Electronic Structure Methods*; Gaussian, Inc.: Pittsburgh, PA, 1996; pp 166−168. McQuarrie, D. A. *Statistical Thermodynamics*; Harper and Row: New York, 1973; Chapter 8.

(24) Baboul, A. G.; Schlegel, H. B. *J. Chem. Phys.* **1997**, *107*, 9413.

(25) Lynch, B. J.; Fast, P. L.; Harris, M.; Truhlar, D. G. *J. Phys. Chem. A* **2000**, *104*, 4811.

(26) Kang, J. K.; Musgrave, C. B. *J. Chem. Phys.* **2001**, *115*, 11040.

(27) Coester, F.; Kümmel, H. *Nucl. Phys.* **1960**, *17*, 477. Cízek, J. *J. Chem. Phys.* **1966**, *45*, 650−654.

(28) Frisch, M. J.; Trucks, G. W.; Schlegel, H. B.; Scuseria, G. E.; Robb, M. A.; Cheeseman, J. R.; Montgomery, J. A., Jr.; Vreven, T.; Kudin, K. N.; Burant, J. C.; Millam, J. M.; Iyengar, S. S.; Tomasi, J.; Barone, V.; Mennucci, B.; Cossi, M.; Scalmani, G.; Rega, N.; Petersson, G. A.; Nakatsuji, H.; Hada, M.; Ehara, M.; Toyota, K.; Fukuda, R.; Hasegawa, J.; Ishida, M.; Nakajima, T.; Honda, Y.; Kitao, O.; Nakai, H.; Klene, M.; Li, X.; Knox, J. E.; Hratchian, H. P.; Cross, J. B.; Adamo, C.; Jaramillo, J.; Gomperts, R.; Stratmann, R. E.; Yazyev, O.; Austin, A. J.; Cammi, R.; Pomelli, C.; Ochterski, J. W.; Ayala, P. Y.; Morokuma, K.; Voth, G. A.; Salvador, P.; Dannenberg, J. J.; Zakrzewski, V. G.; Dapprich, S.; Daniels, A. D.; Strain, M. C.; Farkas, O.; Malick, D. K.; Rabuck, A. D.; Raghavachari, K.; Foresman, J. B.; Ortiz, J. V.; Cui, Q.; Baboul, A. G.; Clifford, S.; Cioslowski, J.; Stefanov, B. B.; Liu, G.; Liashenko, A.; Piskorz, P.; Komaromi, I.; Martin, R. L.; Fox, D. J.; Keith, T.; Al-Laham, M. A.; Peng, C. Y.; Nanayakkara, A.; Challacombe, M.; Gill, P. M. W.; Johnson, B.; Chen, W.; Wong, M. W.; Gonzalez, C.; Pople, J. A. *Gaussian 03*; Gaussian, Inc.: Pittsburgh, PA, 2003.

(29) Sosa, C.; Schlegel, H. B. *J. Am. Chem. Soc.* **1987**, *109*, 4193−4198.

(30) Davey, J. B.; Greenslade, M. E.; Marshall, M. D.; Lester, M. J.; Wheeler, M. D. *J. Chem. Phys.* **2004**, *121*, 3009−3018.

(31) Lee, J.; Bozzelli, J. W. *Int. J. Chem. Kinet.* **2003**, *35*, 20−44.

(32) Kanofsky, J. R.; Lucas, D.; Pruss, F.; Gutman, D. *J. Phys. Chem.* **1974**, *78*, 311−316. Hack, W.; Hoyermann, K.; Sievert, R.; Wagner, H. Gg. *Oxid. Commun.* **1983**, *5*, 101.

(33) Carpenter, B. K. *J. Phys. Chem.* **1995**, *99*, 9801.

(34) see for instance: Yamin, J. A. A.; Abu-Nameh, E. S. M. *Am. J. Appl. Sci.* **2007**, *4*, 257−263.